SPATIAL ANALYSIS OF QUANTITATIVE PRECIPITATION FORECAST ACCURACY BASED ON STRUCTURE AMPLITUDE LOCATION (SAL) TECHNIQUE

Abdullah Ali[1], Achmad Rifani[1], Supriatna[2], Yunus Subagyo Swarinoto[1], Umi Sa'adah[3]
[1] Indonesia Agency for Meteorology Climatology and Geophysics (BMKG)
[2] Department of Geography, Universitas Indonesia
[3] Jakarta Meteorological Watch Office BMKG Soekarno-Hatta

e-mail: abdullah.ali@bmkg.go.id

Received: 03-02-2023; Revised: 09-08-2023; Approved: 16-08-2023

Abstract. Quantitative Precipitation Forecast (QPF) is the final product of a short-term forecasting algorithm (nowcasting) based on weather radar data which is widely used in hydrometeorological aspects. The calculation of the accuracy value using point data on a rainfall gauge often causes a double penalty problem because the QPF prediction results are in the form of spatial objects. This study aims to apply object-based spatial verification in analyzing the accuracy of QPF based on the Short Term Ensemble Prediction System (STEPS) algorithm using the Structure Amplitude Location (SAL) technique. The verification process is carried out by calculating the index value of the structure component (S), amplitude (A), and location (L) in the QPF prediction results based on the results of weather radar observations. The index values for components S and A have a range of -2 to 2, and 0 to 1 for component L with a perfect value of 0. The case study used is the occurrence of heavy rains that caused flooding in Bogor Regency in 2020. SAL verification results from 26 case studies used shows the average value of the components S, A, and L, respectively 0.51, 0.38, and 0.21. As many as 75% of all case studies have S and L component values less than 0.5 which indicate the structure and location of the QPF prediction object is close to the structure and location of the object of observation. A positive value in component A indicates that the QPF prediction results based on the STEPS algorithm tend to be overestimated but on a low scale, namely 0.38 out of 2.

Keywords: *weather radar, QPF, SAL, STEPS*

1 INTRODUCTION

Quantitative Precipitation Forecast (QPF) are widely used in various aspects of hydrometeorology, especially those related to early warning systems (Ali et al., 2022a; Ali et al., 2022b). In general, QPF is an accumulated product of the output of weather radar-based short-term prediction (nowcasting) algorithms (Ali et al., 2021b). The basic methods used to generate predictions range from extrapolation to the application of machine learning. Research institutions in the United States such as the Meteorological Development Lab (MDL), the National Center for Atmospheric Research (NCAR), and the National Severe Storm Laboratory (NSSL) have developed several nowcasting algorithms such as the System for Convection Analysis and Nowcasting (SCAN) (Smith et al., 1998), Warning Decision Support System Integrated Information (WDSS-II) (Hondl et al., 2007) and Auto-Nowcaster (ANC) (Wilson et al., 1998). In England, the United Kingdom Met Office (UKMO) developed the Generating Advanced Nowcast for Deployment in Operational Land Surface Flood (GANDOLF) and Nowcasting and Intialization for Modeling Using Regional Observation Data System (NIMROD) systems by combining numerical prediction models and weather radar data (Pierce et al. al., 2000; Golding., 1998). In Asia, several countries have developed a nowcasting system, including the Japan Meteorological Agency (JMA) with High-Resolution Precipitation Nowcast (HRPN) (Kigawa et al., 2016), Hongkong Observatory with Short-range Warning of Intense Rainstorms in Localized Systems (SWIRLS) (Wong et al., 2006; Yeung, 2012). In Indonesia, BMKG has implemented the Short Term Ensemble Prediction System (STEPS) algorithm in an early warning system that is used to generate predictions for up to 3 hours based on weather radar data (Ali et al., 2021a, Ali et al., 2022c)

The calculation of the accuracy often experiences a double-penalty when the verification technique used is grid-point based (Jolliffe and Stephenson, 2003). When the prediction results are not detected at an observation point, the error value will automatically increase, while the QPF prediction results are only a few kilometers from the observation point (Wernli et al., 2009). These conditions have encouraged many researchers to develop object-based spatial verification methods that consider the various characteristics of the predicted object (Radanovic et al., 2018).

One of the spatial verification techniques that is often used to measure the accuracy of precipitation prediction is the Structure Amplitude Location (SAL) method developed by Wernli et al (2009). This method compares the predicted results with observed values through three components, namely structure (S), amplitude (A), and location (L). The A component is the total precipitation value in all predicted domains, the S component is the size and shape of the predicted precipitation object, and the L component is the predicted location. SAL verification method is rarely used in BMKG weather radar product evaluation, but can avoid double penalty problem from traditional verification method. This study aims to implement object-based spatial verification in analyzing the accuracy of the QPF results from the STEPS- algorithm using the SAL verification technique.

2 MATERIALS AND METHODOLOGY

The case study used in this research is the occurrence of heavy rains that cause flooding in Bogor Regency during 2020. Data of flood events in Bogor Regency is sourced from BPBD Bogor Regency. BMKG weather radar data in Tangerang which has been filtered by interference (Ali et al., 2021) is used to run the STEPS algorithm and accumulated into a QPF in each 70 case study of flood events from previous research (Ali et al., 2022). The QPF calculation using the STEPS algorithm is based on the research results of Pulkkinen et al., (2020) and Ali et al., (2021).

The SAL verification technique was chosen according to the research by Wernli (2008) and Gofa (2018). There are three components that are calculated in the SAL verification method, namely component S, component A, and component L. Components S and A have a value range of -2 to 2, with a perfect score of 0, which means that the predicted results are exactly the same as the observed values (Wernli et al., 2009). In component A, a positive value means the prediction result is overestimated, whereas a negative value means the prediction result is underestimated (Wernli et al., 2009). The calculation of component A is done based on equation 1.

$$A = \frac{\overline{rr_{mod}} - \overline{rr_{obs}}}{0{,}5(\overline{rr_{mod}} + \overline{rr_{obs}})} \qquad [1]$$

mod : model/QPF
obs : observation
$\overline{rr}$: precipitation domain (average)

In the S component, a positive value means that the predicted structure has a wider shape, while a negative value means that the predicted structure has a more localized shape (Wernli et al., 2009). The S component is calculated based on equations 2 and 3.

$$S = \frac{V_{mod} - V_{obs}}{0{,}5(V_{mod} + V_{obs})} \qquad [2]$$

with

$$V = \frac{\sum_i \left(rr_i \frac{rr_i}{rr_i^{max}} \right)}{\sum_i rr_i} \qquad [3]$$

rr_i : total precipitation in entire grid of i object.
rr_i^{max} : maximum value of precipitation in entire grid of i object

The L component has a range of values from 0 to 1, with a perfect value of 0. When the value of the L component is 0, the location of the center of mass predicted is identical to the observed value, and the greater the value of the L component, the location of the center of the predicted mass is farther from the center location observation value period. The calculation of the L component is based on equations 4, 5 and 6.

$$L = L_1 + L_2 \quad [4]$$

with

$$L_1 = \frac{|x(rr_{mod}) - x(rr_{obs})|}{d} \quad [5]$$

$$L_2 = 2\left[\frac{\left|\left(\frac{\sum_i rr_i|x_i - x|}{\sum_i rr_i}\right)_{mod} - \left(\frac{\sum_i rr_i|x_i - x|}{\sum_i rr_i}\right)_{obs}\right|}{d}\right] \quad [6]$$

x_i : center of mass on object i
d : the largest distance between the STEPS prediction domain and the observation domain

Conceptually, examples of FALSE verification results for several combinations of the three components are shown in Figure 2-1.

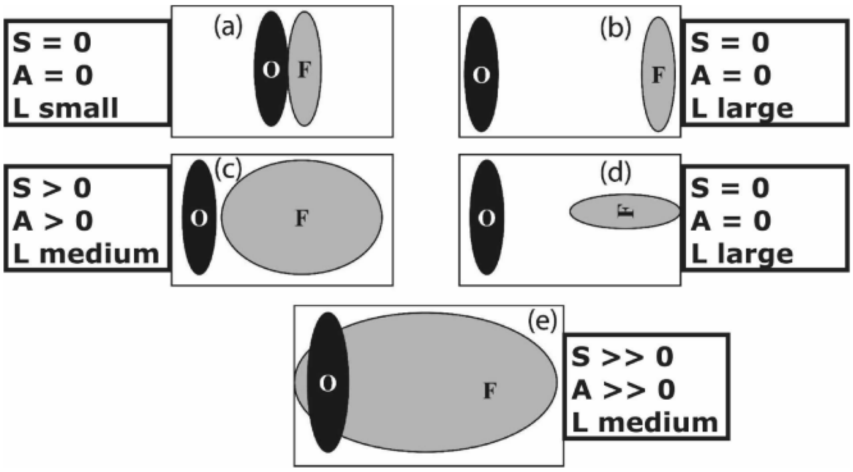

Figure 2-1: Conceptual scheme of the combination of S, A and L components in the SAL spatial verification technique (Wernli et al. 2009)

3 RESULTS AND DISCUSSION

3.1. Ensemble Prediction Results based on STEPS Algorithm

All data on each elevation/sweep of the Tangerang weather radar is used in the STEPS algorithm to generate QPF predictions. The maximum observation distance of the weather radar used is 220 km from the location of the weather radar. The Column Maximum (CMAX) product is used as input for the STEPS algorithm with a data sequence of 120 minutes. The number of ensemble members used in this study is less than the number of ensemble members suggested in the research results of Pulkkinen et al., (2020) (48 ensemble members) this is due to the limitations of the computational resource. Increasing the number of ensemble members has consequences for increasing the ability of the computing system used, so that in this study the number of ensemble members used is reduced to 20 members.

There are significant differences in the prediction results for statiform and convective cloud types. The difference in the predicted results of the STEPS algorithm on stratiform and convective clouds can be seen in Figure 3-1 and 3-2. Statiform clouds have the weather radar echo characteristics with a large area, moderate reflectivity value, and occur for a long duration. While convective clouds have higher reflectivity but occur in a smaller area with a shorter duration. In stratiform cloud types, the STEPS algorithm produces predictions of increasing reflectivity values with an expanding area in each prediction time steps. Whereas in convective clouds, the STEPS algorithm produces slowly decreasing reflectivity in each prediction time steps.

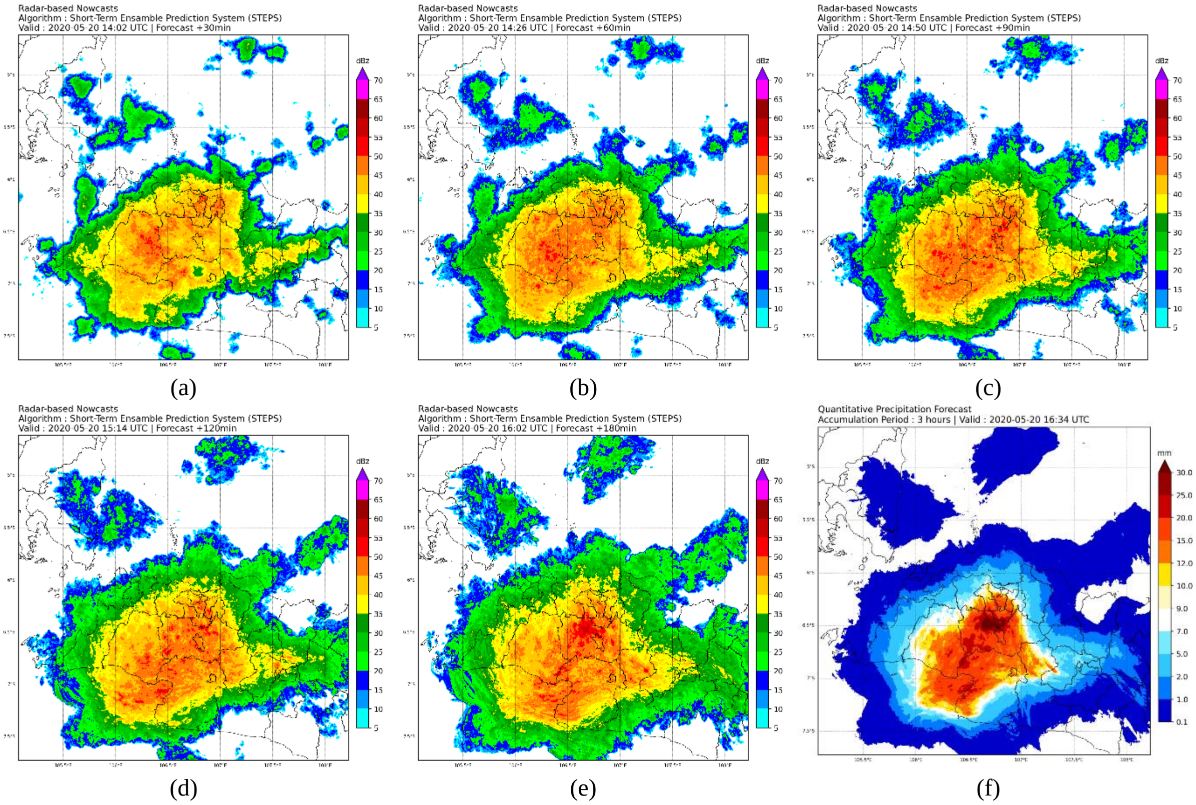

Figure 3-1: Prediction results of the STEPS algorithm on stratiform clouds. Prediction steps: (a) +30 minutes. (b) +60 minutes (c) +90 minutes (d) +120 minutes (e) +180 minutes (f) Accumulated QPF.

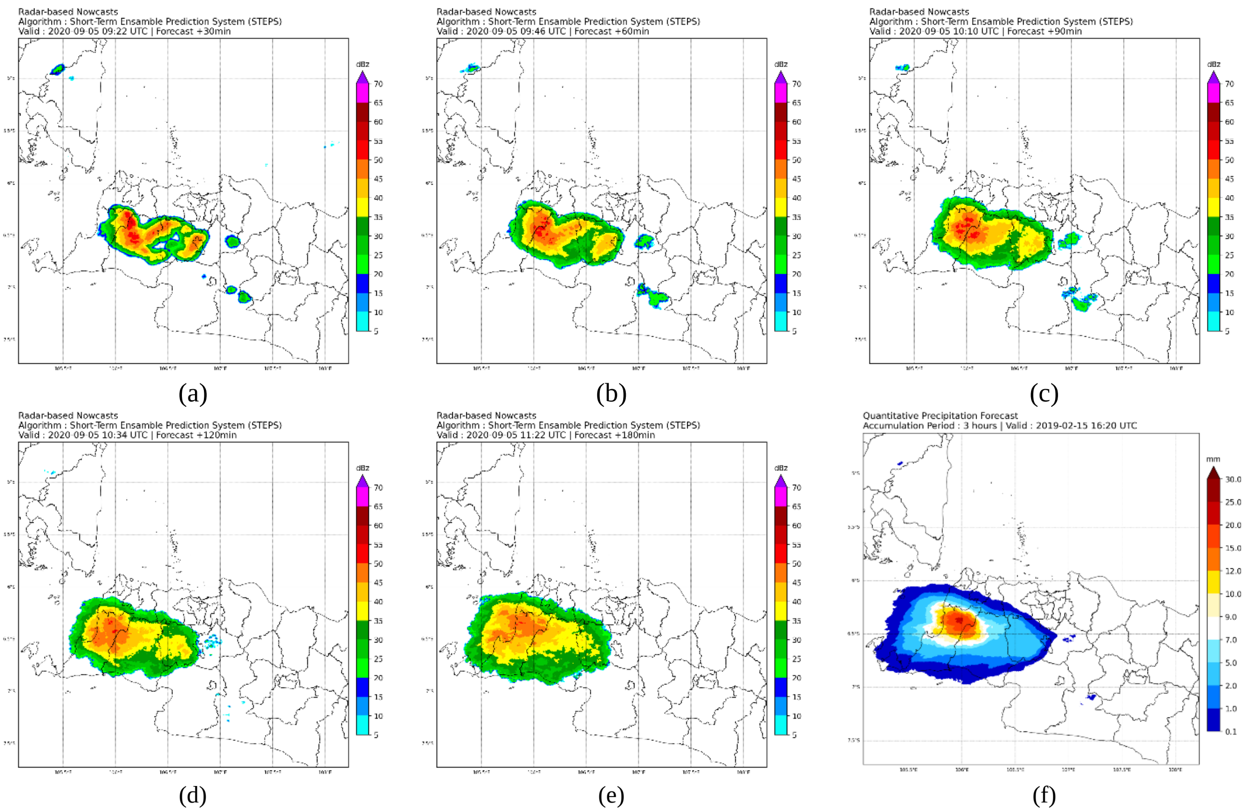

Figure 3-2: Prediction results of the STEPS algorithm on convective clouds. Prediction steps: (a) +30 minutes. (b) +60 minutes (c) +90 minutes (d) +120 minutes (e) +180 minutes (f) Accumulated QPF.

3.2. QPF Spatial Analysis

Spatial analysis of the QPF calculation results was also carried out based on the possible patterns of structure, amplitude, and location in Figure I (Gofa et al., 2018; Wernli et al., 2009). Figure 3-3 shows the results of the QPF with a widened structure pattern and adjacent mass center locations, while in Figure 3-4, the QPF prediction results have a smaller structure than the observed value. One of the weaknesses in the STEPS algorithm is the inability to predict new cloud cells. Figure 3-5 is a case study where a new cloud cell that appears cannot be predicted by the STEPS algorithm, marked with an area in the black box.

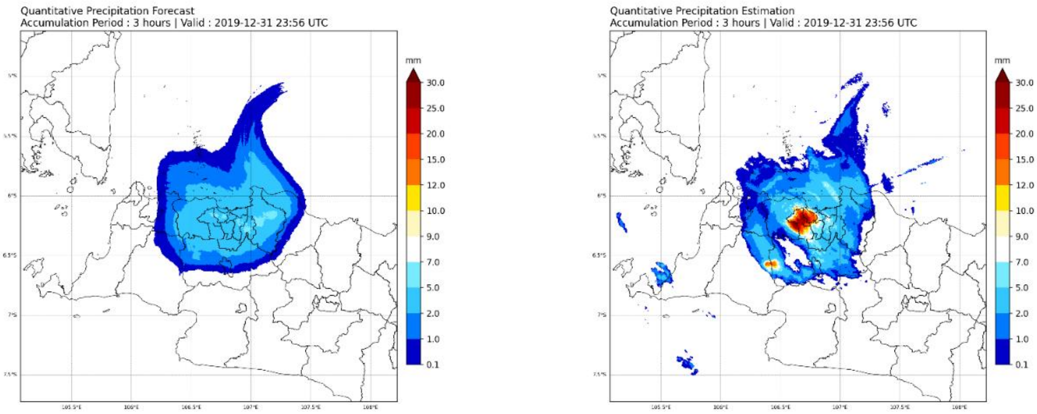

Figure 3-3: QPF results with a widened structure pattern and adjacent mass center locations. (left) Predictions. (right) Observation

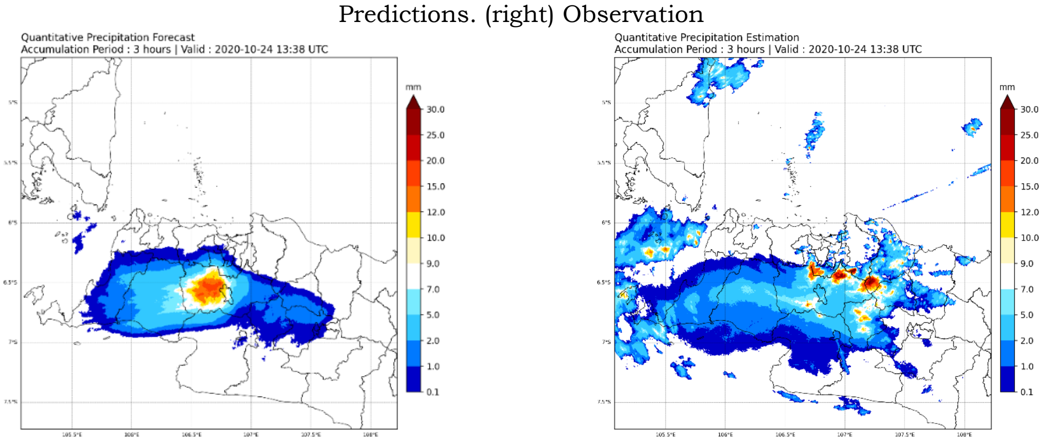

Figure 3-4: QPF results with a structure pattern that is smaller than the observed value. (left) Predictions. (right) Observation

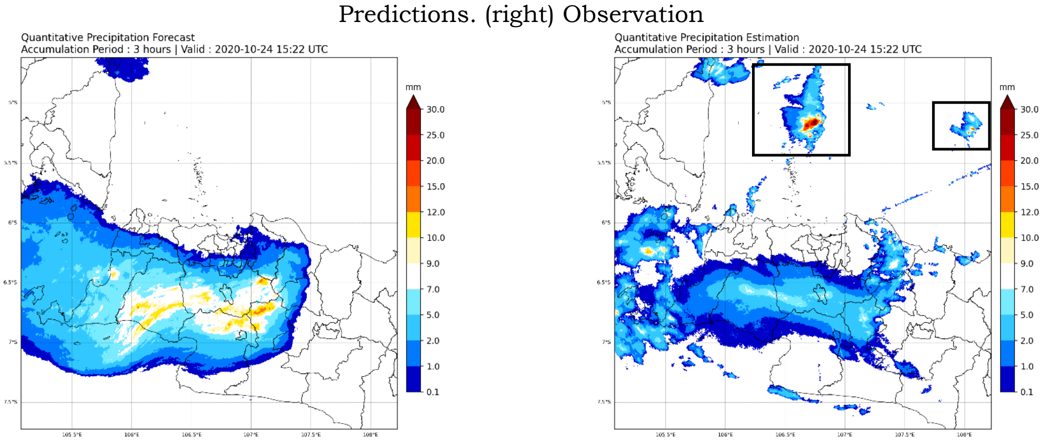

Figure 3-5: QPF results where the STEPS algorithm is unable to predict new cloud cells. (left) Predictions. (right) Observation. The black box in (b) is a new obstacle that cannot be predicted by the STEPS algorithm.

3.3. SAL Verification

The SAL verification results are represented in the SAL diagram and statistics on the elements of structure, amplitude, and location in all case studies are shown in Figure 3-6. In the SAL diagram of Figure 3-6(a), the yellow box represents the 75th percentile of the elements of structure and amplitude. Based on SAL verification statistics, the median value, upper whisker, lower whisker for the S component is 0.55, 1.96, and -1.17 respectively, for the A component is 0.39, 1.99, -1, respectively. 41, and the L component respectively 0.17, 0.62, 0.01. A very high value of component A component occurs in flood events caused by stratiform clouds, where the STEPS algorithm provides predictive results for cloud systems that are strengthened and cause the accumulated value of the QPF to be very high. Likewise in case studies with high S component values due to prediction results with widened objects.

The average values for the S, A, and L components were 0.51, 0.38, and 0.21, respectively. As many as 75% of all case studies have S and L component values of less than 0.5 which indicates the structure and location of the QPF prediction object is close to the structure and location of the observed object. The distribution of object structures is relatively wide from the observed values but on a small scale. A positive value for component A indicates that the QPF prediction results based on the STEPS algorithm tend to be overestimated, but on a low scale, namely 0.39 out of 2. A very low L component value indicates that the difference in distance between the center of the predicted object and the observed object is very small, indicating the location of the object. predictions and objects of observation are almost the same.

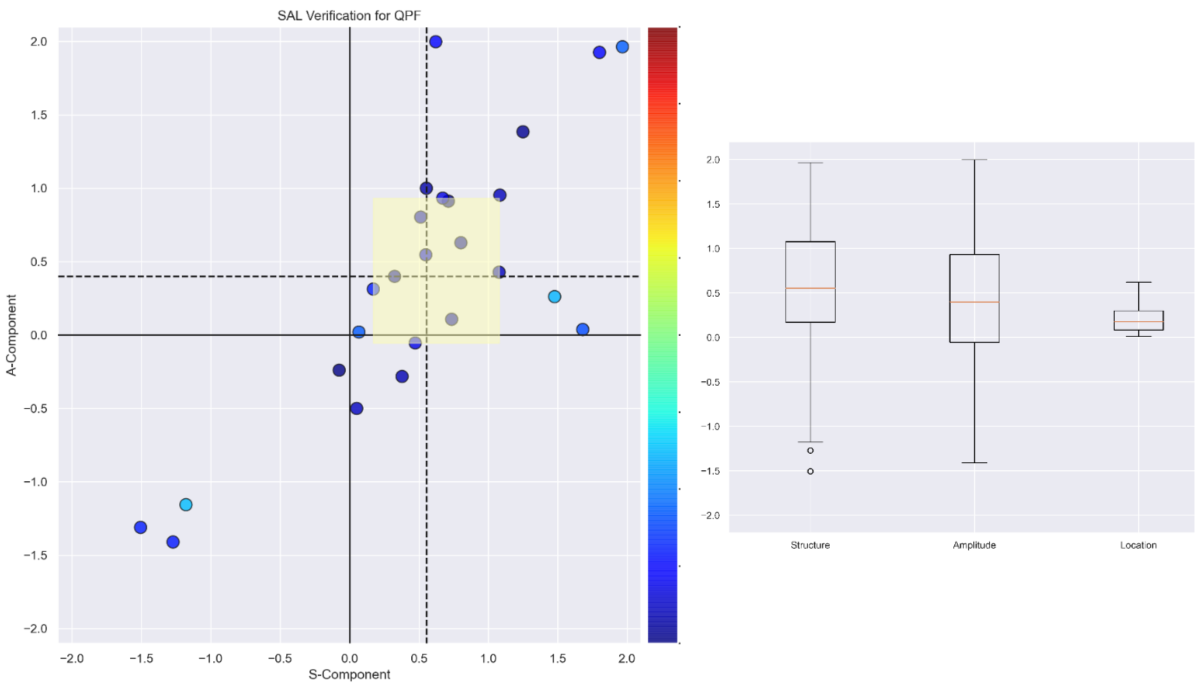

(a) (b)

Figure 3-6: (a) SAL diagram (b) Box plot of S, A, and L components in all case studies.

4 CONCLUSIONS

Analysis of the level of accuracy of the QPF can be carried out using the SAL verification technique. This object-based verification technique spatially analyzes the predicted object with the observed object. The level of accuracy is represented based on the value of the structure (S), amplitude (A), and location (L) components. Based on the flood event case studies used in this study, the SAL verification results show the average values of the S, A, and L components respectively 0.51, 0.38, and 0.21, and as much as 75% of all case studies has an S and L component value of less than 0.5 which indicates that the structure and location of the predicted object are very close to the observed object. The prediction results are relatively overestimated but on a low scale (0.38 out of 2).

Object-based verification techniques are more appropriate for verifying spatial data than conventional verification techniques such as dichotomous. The SAL verification technique can avoid the possibility of a double penalty from the dichotomous verification results, so that the analysis of the accuracy of spatial data becomes more comprehensive.

ACKNOWLEDGEMENTS

The data of this research is fully supported by BMKG Weather Radar Data Management Subdivision. The paper was improved by the helpful suggestion of Dr. Hidde Leijnse from KNMI Netherland. The authors wish to thank all persons who helped this research.

AUTHOR CONTRIBUTIONS

Lead author: Abdullah Ali. Co-Author: Achmad Rifani, Yunus Subagyo Swarinoto, Supriatna, Umi Sa'adah.

Author contributions are as follows: Abdullah Ali: weather radar data processing, nowcasting method, SAL verification, results and analysis. Yunus Subagyo Swarinoto and Supriatna: conceptualization and methodology. Achmad Rifani: SAL verification. Umi Sa'adah: Provision of Tangerang weather radar data.

REFERENCES

Ali, A., Adrianto, R., & Saepudin, M. (2018). Preliminary Study of Horizontal and Vertical Wind Profile of Quasi-Linear Convective Utilizing Weather Radar over Western Java Region, Indonesia. International Journal of Remote Sensing and Earth Sciences (IJReSES), 15(2), 177-186.

Ali, A., Deranadyan, G., & Umam, I. H. (2020). An Enhancement to The Quantitative Precipitation Estimation Using Radar-Gauge Merging. International Journal of Remote Sensing and Earth Sciences (IJReSES), 17(1), 65-74.

Ali, A., Supriatna, S., & Sa'adah, U. (2021a). Radar-Based Stochastic Precipitation Nowcasting Using The Short-Term Ensemble Prediction System (STEPS)(Case Study: Pangkalan Bun Weather Radar). International Journal of Remote Sensing and Earth Sciences (IJReSES), 18(1), 91-102.

Ali, A., Deranadyan, G., & Sa'adah, U. (2021b). Kajian Awal Pemanfaatan Data Penginderaan Jauh dalam Implementasi Peringatan Dini Cuaca Esktrem Berbasis Dampak. Prosiding WIN-ID, 1, 27-36.

Ali, A., Umam, I. H., Leijnse, H., & Sa'adah, U. (2021c). Preliminary Study of A Radio Frequency Interference Filter for Non-Polarimetric C-Band Weather Radar in Indonesia (Case Study: Tangerang Weather Radar). International Journal of Remote Sensing and Earth Sciences (IJReSES), 18(2), 189-202.

Ali, A., Muaya, M., & Kristianto, A. (2022a). Identifikasi Evolusi dan Prediksi Pergerakan Awan Konvektif Berbasis Perangkat Lunak TITAN. Jurnal Ilmiah Geomatika Vol. 28(2), 101-112.

Ali, A., Umam, I. H., Heningtyas, H., Charolidya, R., Sanditya, B., Cempaka, A. P., Teguh Setyawan & Kiki. (2022b). Pengembangan Sistem Peringatan Dini Cuaca Ekstrem Terintegrasi Berbasis Y-Model Webgis Development Methodology (Y-WDM). Jurnal Geografi dan Edukasi Lingkungan (JGEL). Vol.6 No.2 87-100

Ali, A., & Sa'adah, U. (2022c). Implementasi Metode Deteksi Hujan Es Berbasis Data Radar Cuaca Menggunakan Algoritma Severe Hail Index (SHI). Jurnal Fisika Unand, 11(3), 380-386.

Ali, A., Swarinoto, Y. S., & Sa'adah, U. (2022d). Penentuan Nilai Batas Ambang Akumulasi Curah Hujan pada Kejadian Banjir di Kabupaten Bogor Berbasis Data Radar Cuaca. Jurnal Aplikasi Meteorologi, 1(2).

Gofa, F., Boucouvala, D., Louka, P., & Flocas, H. A. (2018). Spatial Verification Approaches As A Tool to

Evaluate The Performance of High Resolution Precipitation Forecasts. Atmospheric Research, 208, 78-87.

Golding, B. W. (1998). Nimrod: A System for Generating Automated Very Short Range Forecasts. Meteorological Applications, 5(1), 1-16.

Hidayat, A. M., Aofany, D., Arfianti, D. R., Nugraheni, I. R., & Ali, A. (2019). Prediksi Intensitas Curah Hujan Menggunakan Produk *Nowcasting* Rtr Dibandingkan dengan Produk Estimasi Curah Hujan Sri pada Kejadian Banjir di Palembang Tanggal 12–13 November 2018. Jurnal Meteorologi Klimatologi dan Geofisika, 6(1), 1-12.

Hondl, K. D., Lakshmanan, V., Smith, T. M., & Stumpf, G. J. (2007, January). Warning Decision Support System-Integrated Information (WDSS-II) Progress and Plans. In Extended Abstracts, 23rd Conf. on Interactive Information Processing Sys.

Kigawa, S., Hayashi, T., & Nishimura, T. (2016). Advanced Weather Radar Application Technology at JMA. WMO/CIMO/TECO-2016, Madrid, Spain, 27-29 September.

Pierce, C. E., Hardaker, P. J., Collier, C. G., & Haggett, C. M. (2000). GANDOLF: A System for Generating Automated Nowcasts of Convective Precipitation. Meteorological Applications, 7(4), 341-360.

Pulkkinen, S., Chandrasekar, V., von Lerber, A., & Harri, A. M. (2020). Nowcasting of Convective Rainfall Using Volumetric Radar Observations. IEEE Transactions on Geoscience and Remote Sensing, 58(11), 7845-7859.

Radanovics, S., Vidal, J. P., & Sauquet, E. (2018). Spatial Verification of Ensemble Precipitation: An Ensemble Version of SAL. Weather and Forecasting, 33(4), 1001-1020.

Smith, S. B (1998). The System for Convection Analysis and Nowcasting (SCAN). Preprints, 16th Conf. on Weather Analysis and Forecasting, Phoenix, AZ, Amer. Meteor. Soc., J22–J24.

Wernli, H., Paulat, M., Hagen, M., & Frei, C. (2009). SAL—A Novel Quality Measure for the Verification of Quantitative Precipitation Forecasts. Monthly Weather Review, 136(11), 4470-4487.

Wilson, J. W., Crook, N. A., Mueller, C. K., Sun, J., & Dixon, M. (1998). Nowcasting Thunderstorms: A status report. Bulletin of the American Meteorological Society, 79(10), 2079-2100.

Wong, W. K., & Lai, E. S. T. (2006). RAPIDS–Operational Blending of Nowcast and NWP QPF. In 2nd International Symposium on Quantitative Precipitation Forecasting and Hydrology, Boulder, USA (pp. 4-8).

Yeung, H. Y. (2012). Recent Developments and Applications of the SWIRLS Nowcasting System in Hong Kong. In The 3rd WMO International Symposium on Nowcasting and Very Short-Range Forecasting (pp. 6-10).